

## Tumor microtubes convey resistance to surgical lesions and chemotherapy in gliomas

Sophie Weil, Matthias Osswald, Gergely Solecki, Julia Grosch, Erik Jung, Dieter Lemke, Miriam Ratliff, Daniel Hänggi, Wolfgang Wick, and Frank Winkler

*Neurology Clinic and National Center for Tumor Diseases, University Hospital Heidelberg, Heidelberg, Germany (S.W., M.O., G.S., J.G., E.J., D.L., W.W., F.W.); Clinical Cooperation Unit Neurooncology, German Cancer Consortium (DKTK), German Cancer Research Center (DKFZ), Heidelberg, Germany (S.W., M.O., G.S., J.G., E.J., D.L., M.R., W.W., F.W.); Department of Neurosurgery, University Hospital Mannheim, University Heidelberg, Mannheim, Germany (M.R., D.H.)*

**Corresponding Author:** Frank Winkler, MD, PhD; Neurology Clinic, Im Neuenheimer Feld 400, 69120 Heidelberg ([frank.winkler@med.uni-heidelberg.de](mailto:frank.winkler@med.uni-heidelberg.de)).

### Abstract

**Background.** Primary and adaptive resistance against chemo- and radiotherapy and local recurrence after surgery limit the benefits from these standard treatments in glioma patients. Recently we found that glioma cells can extend ultra-long membrane protrusions, “tumor microtubes” (TMs), for brain invasion, proliferation, and interconnection of single cells to a syncytium that is resistant to radiotherapy. We wondered whether TMs also convey resistance to the other 2 standard treatment modalities.

**Methods.** Patient-derived glioblastoma stemlike cell (GBMSC) lines were implanted under a cranial window in mice. Longitudinal in vivo two-photon laser scanning microscopy was used to follow tumor growth, including the fate of single glioma cells over months.

**Results.** After a cylindrical surgical lesion, GBMSCs increasingly extended TMs toward the lesion area, which contributed to the repopulation of this area over many weeks. In fact, an excessive “healing response” was observed in which tumor cell densities significantly exceeded those of unlesioned brain regions over time. Inhibition of TM formation and function by genetic targeting of growth associated protein-43 robustly suppressed this surgery-induced tumor growth reaction, in contrast to standard postsurgical anti-inflammatory treatment with dexamethasone. After one cycle of temozolomide chemotherapy, intra- and intertumoral heterogeneity of TM formation and interconnection was strongly associated with therapy response: when tumor cells were integrated in TM networks, they were more likely to resist chemotherapy.

**Conclusion.** TMs can contribute to the resistance against standard treatment modalities in gliomas. Specific inhibition of TMs is a promising approach to reduce local recurrence after surgery and lower resistance to chemotherapy.

### Key words

chemotherapy | glioma | resistance | surgery | tumor microtubes

Diffuse astrocytomas, including the most aggressive glioblastomas (GBs), are primary brain tumors that cannot be completely resected, and thus remain incurable.<sup>1</sup> Standard treatments consist of surgery, followed by radio- and chemotherapy.<sup>2–4</sup> Despite this intensive treatment, tumor resistance and recurrence limit its efficacy. One major cause for treatment failure is the early and widespread

dissemination of tumor cells, making gliomas a disease of the whole brain.<sup>5,6</sup>

Total surgical tumor resection improves survival in GB patients.<sup>7,8</sup> However, most GBs recur at or around the resection margin, even after gross total resection of the contrast-enhancing tumor mass.<sup>9–11</sup> This recurrence pattern, which is seemingly in contrast to the whole-brain character of the

## Importance of the study

The inevitable recurrence of malignant astrocytomas, including glioblastomas, after standard therapy speaks for the existence of a resistant subpopulation of glioma cells that is not sufficiently targeted by current therapies. Moreover, it is a long-standing observation that the majority of tumors recur at or around the resection margin, despite the diffuse colonization of the entire brain in these diseases. Here we provide a possible explanation by showing that tumor cells extend TMs

toward the surgical lesion site to actively “repair” the damage, leading to a repopulation of the lesioned area that ultimately results in a new tumor mass at this site. In addition, TM-connected glioma cells are more resistant to the cytotoxic effects of temozolomide chemotherapy. Our data suggest that specific interference with TM formation and function, such as targeting growth associated protein-43, can be a novel strategy to fight primary and adaptive resistance in gliomas.

disease, is insufficiently understood. To date, it was mainly explained by the higher density of tumor cells in the direct vicinity of the resected main tumor mass.<sup>12</sup> Consequently, therapeutic strategies to prevent or delay those frequent local recurrences have been developed, most notably the implantation of carmustine wafers into the resection cavity,<sup>13,14</sup> and recently intraoperative radiotherapy (the INTRAGO study<sup>15</sup>). The limited or unknown efficacy and toxicity of those approaches compromise their widespread use in the clinic today.

Temozolomide (TMZ) is the standard alkylating agent used for GB chemotherapy. Despite increasing patient survival, treatment efficacy is limited, as gliomas frequently show primary or adaptive resistance to TMZ therapy.<sup>16</sup> The most important driver of resistance that is known today is the O<sup>6</sup>-methylguanine-DNA methyltransferase (MGMT) protein. MGMT repairs DNA damage caused by TMZ treatment, thereby avoiding tumor cell apoptosis. Thus, gliomas with a lack of MGMT expression due to gene promoter hypermethylation are the ones that respond best to TMZ therapy.<sup>17–20</sup> Nevertheless, there are GBs and other gliomas that do not respond to TMZ despite *MGMT* promoter hypermethylation, and all tumors eventually recur despite TMZ therapy,<sup>21,22</sup> indicating that additional mechanisms of resistance must be involved. New approaches are needed to better sensitize gliomas to TMZ.

One candidate mechanism for treatment resistance in gliomas is the formation of tumor microtubes (TMs). These are ultra-long, thin, and highly dynamic membrane protrusions extended into the surrounding tissue from a subset of astrocytoma cells, used for tumor cell invasion and proliferation, and thereby leading to efficient colonization of the brain.<sup>23</sup> Over time, TMs often connect tumor cells with each other. These TM connections are composed of connexin 43 (Cx43) gap junctions; Cx43 is the most abundant subtype of connexins in the CNS and is predominant in glioblastoma cells.<sup>23</sup> TM-connected tumor cells are more resistant against the detrimental effects of standard radiotherapy, most likely due to improved multicellular homeostasis in the network.<sup>23</sup> So far, one gene critical for TM formation has been identified, growth associated protein-43 (GAP-43), which is normally expressed during neurogenesis<sup>24</sup> and whose expression in gliomas depends on an intact 1p/19q status.<sup>23</sup> GAP-43 is used by tumor cells to extend TMs and to build a functional TM network.<sup>11</sup>

In light of these recent findings, we sought to understand whether TMs (and the different biological aspects

of glioma progression and resistance they are involved in) also contribute to GB resistance to the other 2 standard therapies: surgery and chemotherapy. To answer this question, we used our in vivo 2-photon microscopy mouse model that allows us to follow individual tumor regions and single glioma cells over extended periods of time—but also to interfere with the brain tumor and study its reaction. The findings imply a relevant role of TMs for resistance to standard therapies.

## Materials and Methods

### Cell Culture and Lentiviral Transductions

The primary glioblastoma cell lines S24 and T269 (isocitrate dehydrogenase wild-type, MGMT promoter hypermethylated; GBMSCs) were kept under “stemlike” conditions in spheroid cell culture. Stable transduction with lentiviral vectors allowed in vivo imaging: the LeGO-T2 vector (gift from A. Trumpp) induced cytosolic red fluorescent protein (tdTomato) expression in GBMSCs. Additional transduction with pLKO.1-LV-GFP (Addgene 25999, Elaine Fuchs) vector resulted in nuclear green fluorescent protein (GFP) expression (H2B-GFP). Alternatively, the transduction of GBMSCs with pLenti6.2 hygro/V5-Lifeact-YFP created a yellow fluorescent protein (YFP) signal in actin filaments.

Knockdown of GAP-43 using small hairpin (sh)RNA technology (pLKO.1-puro-CMV-vector, Sigma Aldrich) targeted the sequence TGTAGATGAAACCAAACCTAA. For an appropriate control, the same cell line was transduced with the respective nontargeting shRNA lentivirus (SHC016, Sigma Aldrich). Regular tests for mycoplasma infections were done by PCR and verification of glioblastoma origin was performed by comparative genomic hybridization or 450k analysis.<sup>11,25</sup>

### In Vitro Experiments

For cell viability under TMZ treatment, 7500 cells per well in each of 3 wells were grown in a 96-well plate ( $n = 3$ ). Ninety-six hours after dimethyl sulfoxide control or 10  $\mu$ M TMZ treatment, an assay by MTT (3-(4,5-dimethylthiazol-2-yl)-2,5-diphenyltetrazolium bromide; 1 mg/mL) was performed. The absorbance was read at 590 nm with a reference filter at 620 nm. In vitro S24 and T269 fluorescent

spheroids were transferred into an imaging chamber, and images of the spheroids were acquired using a Leica TCS SP5 microscope.

### Mouse Cranial Window Preparation and Tumor Initiation

For the preparation of *in vivo* experiments, a chronic cranial window was implanted into 8- to 10-week-old male Naval Medical Research Institute nude mice as described before.<sup>23,26,27</sup> At least 10 days after implantation of the chronic cranial window, the glass was temporarily removed to inject 50 000 GBMSCs into the mouse cortex at a depth of 500  $\mu\text{m}$ . All animal procedures were performed in accordance with the institutional laboratory animal research guidelines after approval by the Regierungspräsidium Karlsruhe, Germany (G188-12, G132-16).

### Surgical Lesion, Dexamethasone Treatment, and Chemotherapy

For surgical lesion experiments, the chronic cranial window was removed, and a 26-gauge needle-bearing Hamilton syringe was used to resect a defined cylindrical volume of approximately 300  $\mu\text{m}$  diameter out of a long-term imaged, tumor cell-bearing mouse brain area of 1154  $\times$  1154  $\mu\text{m}$ . For all treatments, we waited for the establishment of malignant gliomas of a relevant size and cellular density; these tumors also displayed cellular heterogeneity regarding TM formation and interconnection. For chemotherapy experiments, mice were treated on D85  $\pm$  3 after tumor injection with 100 mg/kg body weight (bw) TMZ *p.o.* for 3 consecutive days (D0, 1, 2), without prior surgical lesion. For dexamethasone (DEX) experiments, mice received 0.3 mg/kg bw DEX *s.c.* every day for 14 days starting on the day of the surgical lesion.

Mice were evaluated daily for clinical and behavioral abnormalities and sacrificed when they developed neurological deficits or weight loss >20%.

### In Vivo Multiphoton Laser Scanning Microscopy

Multiphoton laser scanning microscopy (MPLSM) was used as described before.<sup>23</sup> A Chameleon Ultra II laser (Coherent) excited the fluorophores through a BP500–550/BP 575–610 filter. For detection of the GFP- and injected tetramethylrhodamine-isothiocyanate–Dextran, the laser wavelength was set to 850 nm. Tuning to 950 nm allowed the measurement of tdTomato, LifeActYFP, and fluorescein isothiocyanate–Dextran.

### Image Processing

After data acquisition by Zeiss ZEN software, images were prepared for analysis. Tiles were stitched, image calculation cleared unspecific background, and cropping allowed exact comparison of longitudinally acquired data. Images shown here were processed in Imaris (Bitplane) by filtering and subtracting background, and saved in 3D

(surgical lesion experiments) or orthogonal view (chemotherapy experiments).

### Quantifications

Analysis of images was performed with the ImageJ (National Institutes of Health) and Imaris (Bitplane) software. Cells were counted manually in ImageJ.

### Statistics

SigmaPlot Software (Systat Software) was used for statistical analysis of the quantifications.

For detailed material and methods, see the Supplementary material.

## Results

### Surgical Lesions Are Excessively Repopulated by Glioblastoma Cells Over Time

To better understand the mechanisms of GB recurrence after surgical resection, we used an *in vivo* mouse model that allows longitudinal imaging of brain tumor progression, and response to interventions, in the live mouse brain.<sup>23,27,28</sup> Two primary human GBMSC lines (S24 and T269) representative for the human disease<sup>23</sup> were chosen.

After surgical removal of a cylindrical brain tissue volume colonized by GBMSCs, glioblastoma cells repopulated the lesioned area over time (Fig. 1A). This striking response to the surgical trauma resulted in increasing glioblastoma cell densities in the lesioned brain area over a period of weeks, exceeding those of perilesional and distant brain regions (Fig. 1B–C), as well as those of nonresected control animals (Supplementary Figure S1A, B). We next aimed to identify the cellular mechanisms responsible for this lesion-specific increase in tumor cell content. First the velocity of tumor cell nuclei was determined to investigate whether the trauma had a general impact on tumor cell motility. Indeed, at the time when excessive repopulation of the lesion started (day 5), nuclear velocity was significantly increased in the perilesional area (Fig. 1D). By that time, more than half of the tumor cell nuclei moved directly toward the lesion area (Fig. 1E). When analyzing the larger brain tumor region where the surgical intervention took place, total tumor cell densities were reduced compared with control due to the tissue removal in the days after resection but caught up to control tumors at day 7 (Supplementary Figure S1C). Together these data speak for both increased invasion of perilesional preexisting glioblastoma cells to the resection margin as well as increased tumor cell proliferation in the lesioned brain area after a surgical lesion.

### Tumor Microtubes Are Responsible for the Glioma Repair Response

Next we aimed to investigate whether TMs, with their known ability to replace a lost single member of the tumor

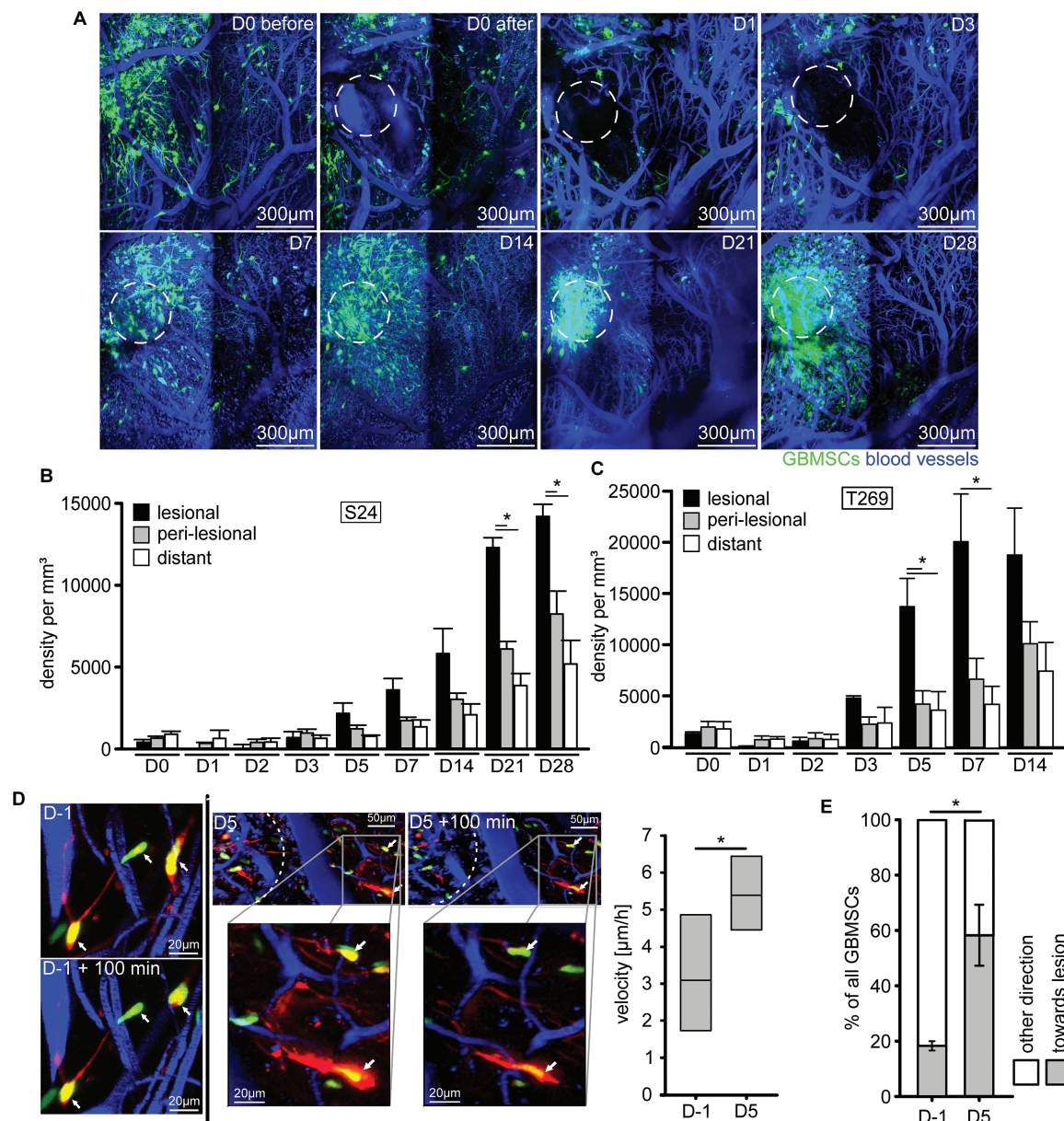


**Fig. 1** Glioblastoma cells excessively repopulate surgical lesions. (A) Representative in vivo MPLSM images of S24 GBMSCs repopulating an area (dotted circle) where a cylindrical volume of tumor cell-bearing brain tissue was surgically removed by a thick needle puncture. D0 before, area just before surgical intervention; D0 after, area just after surgical intervention; D1–D28, time course of repopulation of the lesioned area from day 1 to day 28 after intervention. 3D images, 72–285  $\mu\text{m}$  depth under the brain surface. (B, C) Time course of the density of S24 (B) and T269 (C) GBMSC per  $\text{mm}^3$  within the puncture area (lesional), in the surrounding brain tissue directly adjacent to the lesion (peri-lesional, 0–300  $\mu\text{m}$  from resection margin), and distant brain areas (>300  $\mu\text{m}$  from resection margin) ( $n = 3$  mice, one-way ANOVA). (D) Representative images of T269 GBMSCs migrating toward the lesion on day 5, and corresponding quantification of nuclear velocity increasing 5 days after surgical lesion compared with 1 day before surgery (60 cells from  $n = 3$  mice,  $t$ -test). (E) GBMSCs (T269) migrating toward the lesioned area on day 5 (reduction of a cell's distance to the lesioned area) vs away from the lesioned area (60 cells from  $n = 3$  mice,  $t$ -test). Error bars show standard error of the mean (SEM),  $*P < 0.05$ .

cell network,<sup>23</sup> also contribute to recolonization of a surgical lesion area. Indeed, glioblastoma cells in the vicinity of the resection cavity extended newTMs toward and then into the lesioned area from day 3 on, which preceded recolonization of the former resection cavity with tumor cells (Fig. 2A).

Quantifications revealed that tumor cells of both the S24 and T269 glioma cell lines in the surrounding and more distant brain regions increasingly extendedTMs toward the lesioned area over time (Fig. 2B, C). Even the usually TM-poorer T269 glioblastoma cell line extendedTMs toward the lesion, which

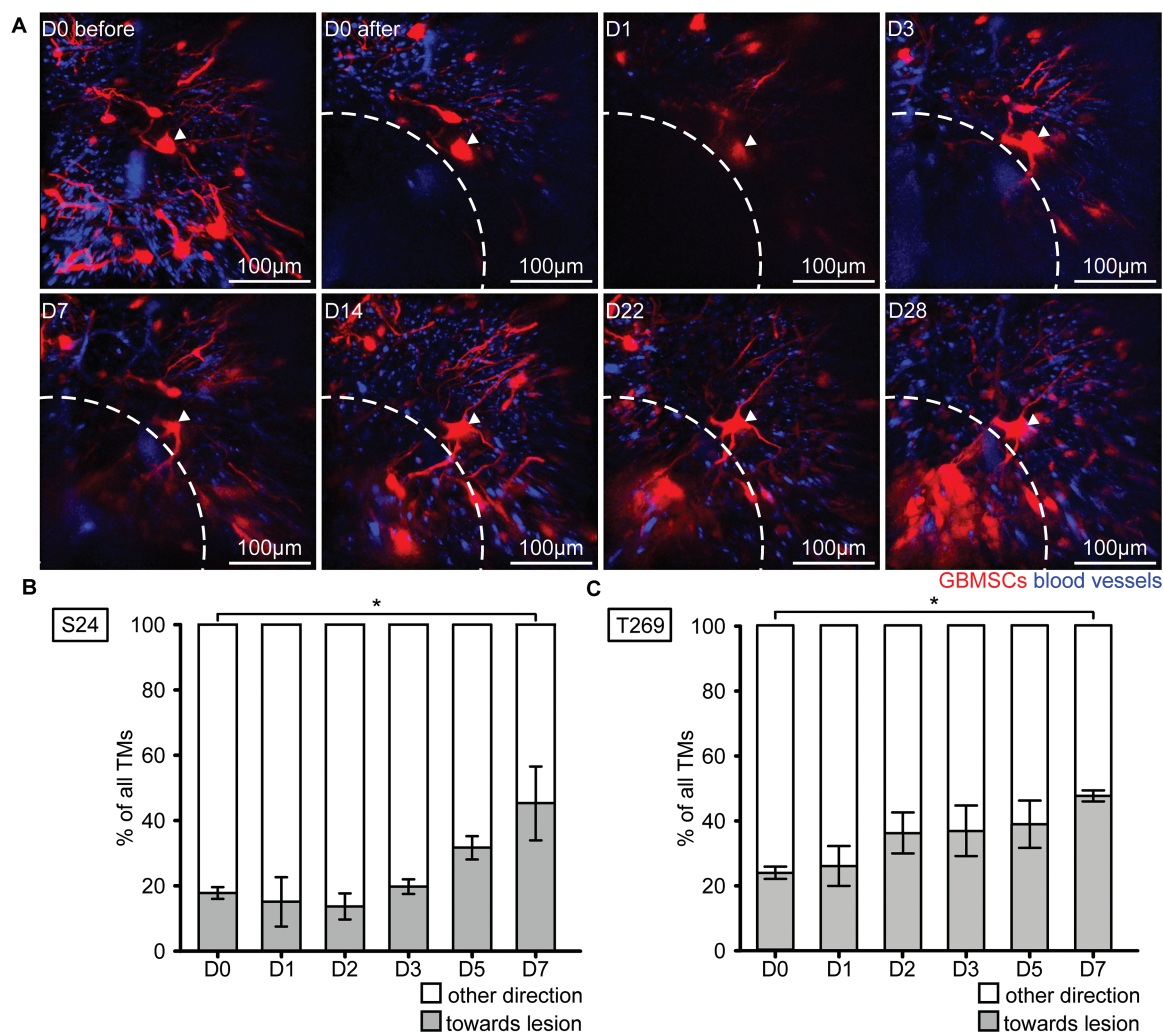


**Fig. 2** Tumor microtubes are extended to the lesioned area. (A) After surgical removal of a tumor cell-bearing brain volume (dotted line), an adjacent S24 GBMSC tumor cell (arrow) extends a long cellular protrusion characteristic of a TM into the resected area from day 3 on. Note that additional new TMs, originating from tumor cells outside the displayed volume and directed toward the lesioned area, can also be found from day 3 on. In vivo MPLSM 3D images, 69–174  $\mu\text{m}$  depth under the brain surface. (B, C) Percentage of TMs extended toward the lesion for S24 (B) and T269 (C) GBMSC lines (S24:  $n = 3$ –143 GBMSCs per day quantified; T269:  $n = 7$ –152 GBMSCs per day quantified;  $n = 3$  mice,  $t$ -test). Error bars show SEM. \* $P < 0.05$ .

could indicate that the processes leading to TM extension are strong enough to even induce TM formation in TM-poor tumors. Together this indicates an involvement of TMs in mediating the repopulation process, in accordance with their previously described role in tumor cell invasion, proliferation, and colonization of the unlesioned brain.<sup>23</sup>

To specifically interrupt TM formation and thus TM-mediated repair response, we implanted GBMSCs with a stable knockdown of GAP-43 by small hairpin RNA (shGAP-43), which leads to compromised TM morphology and function without affecting in vitro viability of the tumor cells.<sup>23</sup> We chose to knock down GAP-43 because shGAP-43 gliomas show highly impaired TM formation and function, including reduced Cx43 expression, leading to reduced TM-dependent tumor invasion and proliferation.<sup>23</sup> In contrast to shControl tumors, shGAP-43 tumors did not show an excessive

population of the lesioned area over many weeks (Fig. 3A). Further quantitative analysis confirmed that the GAP-43 knockdown significantly and specifically inhibited the tumor repair response within and close to the lesioned area from day 5 on (Fig. 3B). Higher magnifications revealed that shGAP-43 tumors were indeed deficient in extending TMs toward the lesioned area and in recolonizing it (Fig. 3C).

### Anti-inflammatory Treatment Has Only Transient Effects on the Repair Response

We next investigated whether anti-inflammatory treatment with DEX, routinely done after surgical resections and biopsies in glioma patients to reduce inflammatory changes, including perioperative edema,<sup>29</sup> has any impact

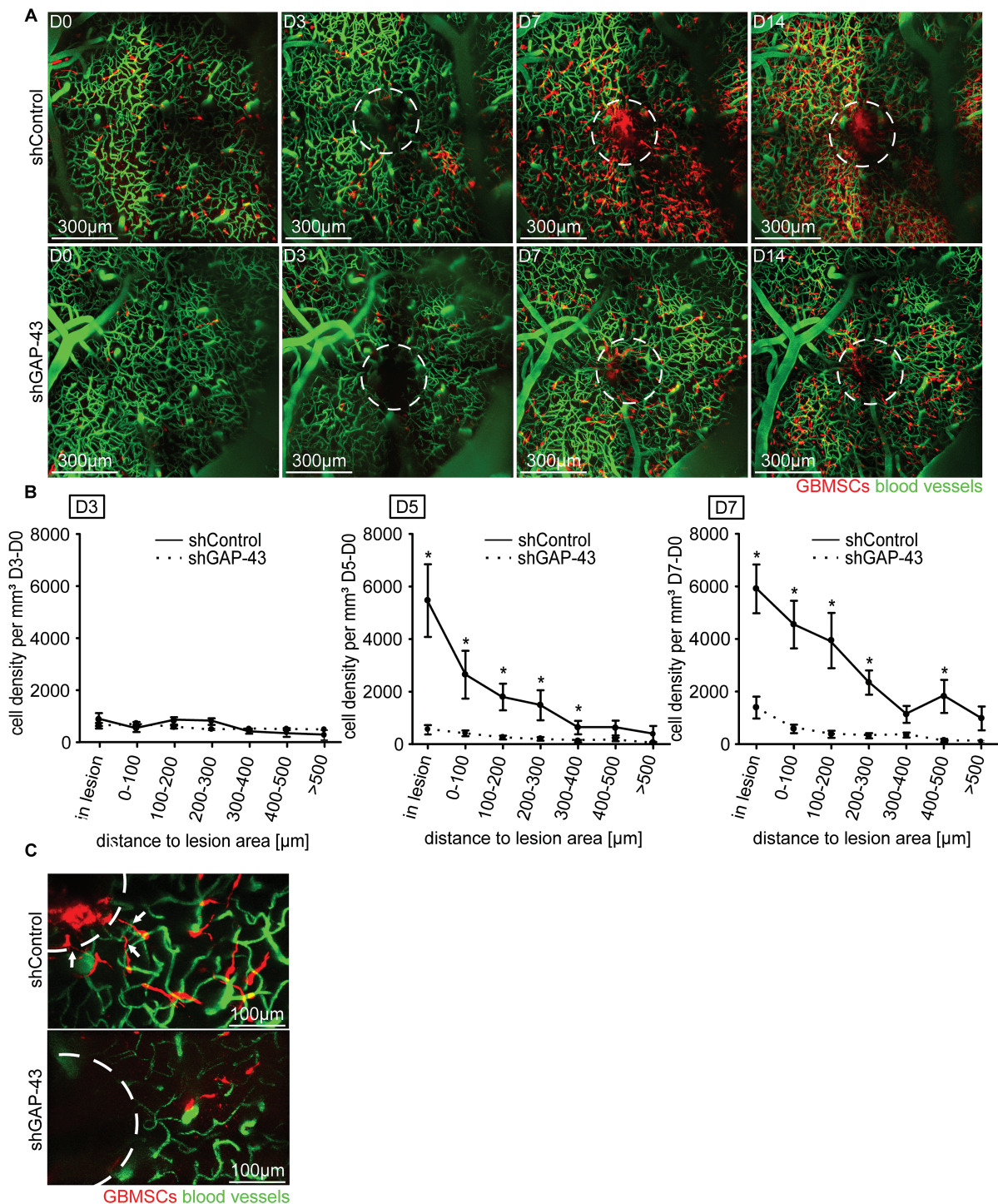


**Fig. 3** GAP-43 deficient glioma cells fail to repopulate surgical lesions. (A) Representative in vivo MPLSM 3D images of the repopulation of lesioned areas (dotted circles) by S24 shControl vs shGAP-43 GBMSCs, up to 14 days after surgical lesion, 75–225  $\mu\text{m}$  depth under the brain surface. (B) Quantification of the tumor cell number in S24 shControl GBMSCs vs S24 shGAP-43 cells over time (9–1467 GBMSCs quantified; 4 regions,  $n = 3$  mice per group,  $t$ -test). (C) Representative in vivo MPLSM image of S24 tumor cells repopulating the lesioned area (dotted circle) in shControl vs shGAP-43 on day 5 after lesion. Note the TMs reaching toward the lesion in shControl and their absence in shGAP-43. Error bars show SEM.  $*P < 0.05$ .

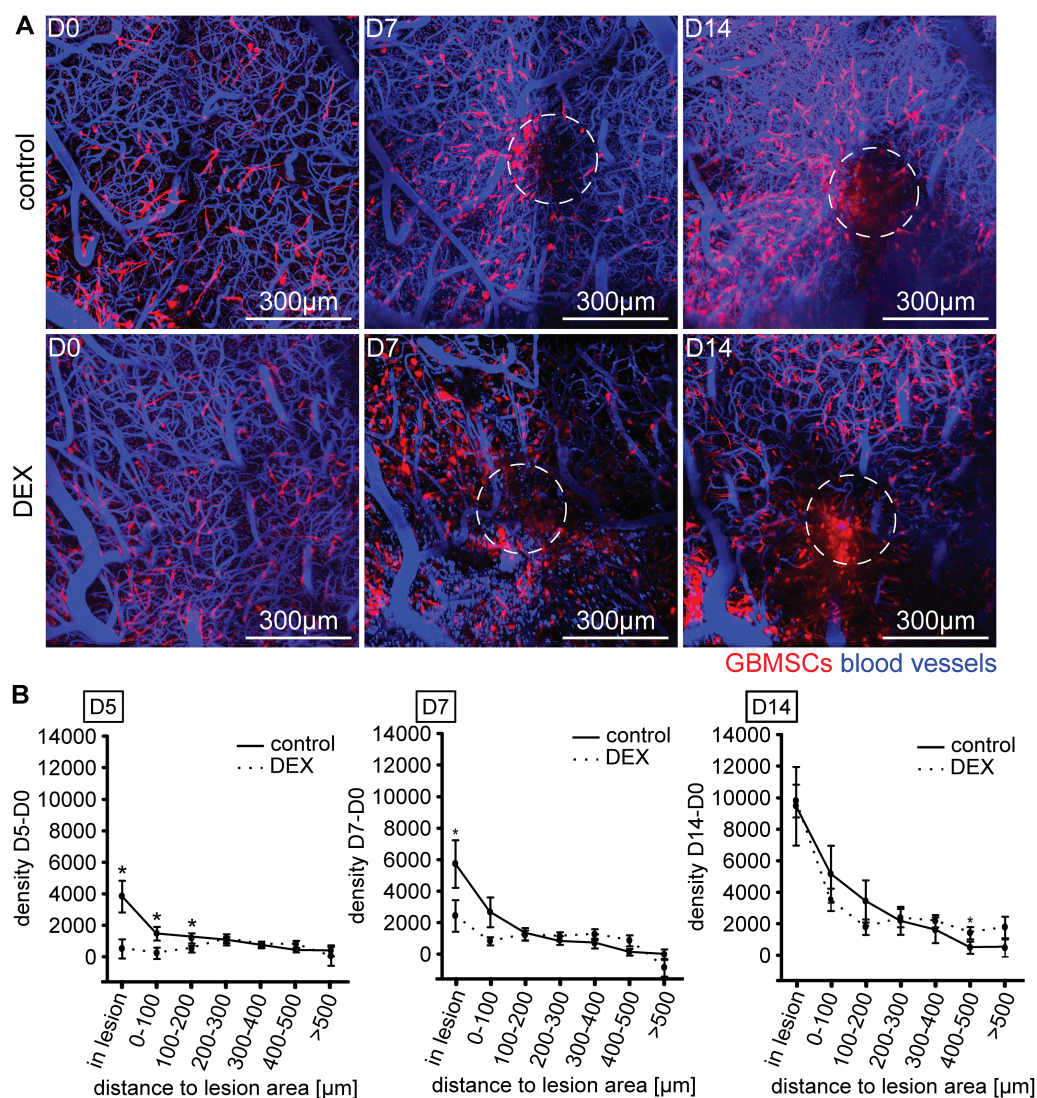


**Fig. 4** Treatment with DEX delays GBMSC accumulation in lesioned areas, but does not prevent it. (A) Representative in vivo MPLSM 3D images of mice implanted with S24 GBMSCs and treated with vehicle control vs DEX (0.3 mg/kg s.c.). Note the decreased formation of a new tumor mass in the lesioned area (dotted circle) at day 7, but similar tumor formations at day 14, 42–195 µm depth under the brain surface. (B) Tumor cell densities in relation to the lesioned area in control vs DEX treated mice on day 5 (left panel), day 7 (middle panel), and day 14 (right panel) postsurgery (43–1653 GBMSCs quantified; 4 regions,  $n = 3$  mice per group,  $t$ -test). Error bars show SEM. \* $P < 0.05$ .

on the remarkable reaction of glioblastoma cells to the surgical lesions. Mice were treated with DEX perioperatively (12 hours before to 14 days after surgery). While there was reduction of tumor cell repopulation of the lesioned area at day 5 and less so at day 7 after the surgical lesion in the DEX treatment group, this reduction was no longer evident by day 14 (Fig. 4A, B). By this time, lesional tumor cell densities in the DEX group had fully caught up to those measured in the control group.

#### Highly TM-Connected Tumors and Glioblastoma Cells Better Resist Chemotherapy

To investigate the effects of TMZ chemotherapy on the survival of individual glioblastoma cells in growing brain

tumors and to clarify whether this survival depends on their extension of TMs and integration into a TM-linked tumor cell network,<sup>23</sup> we treated mice with an established high but tolerable dose of 100 mg/kg TMZ for 3 consecutive days and followed distinct brain regions over prolonged periods of time. We chose 2 *MGMT* promoter hypermethylated GBMSC lines, one growing with dense cell-cell interconnections via TMs in the mouse brain (S24), and one where these interconnections were only infrequently observed (T269) (Fig. 5A–C). Despite the stemlike conditions of in vitro culture, relevant formation of classical TMs was not detectable (Fig. 5D), arguing for an impact of the brain microenvironment on TM formation. Under these TM-free in vitro growth conditions, the viability of the S24 cell line was more reduced by TMZ than that of

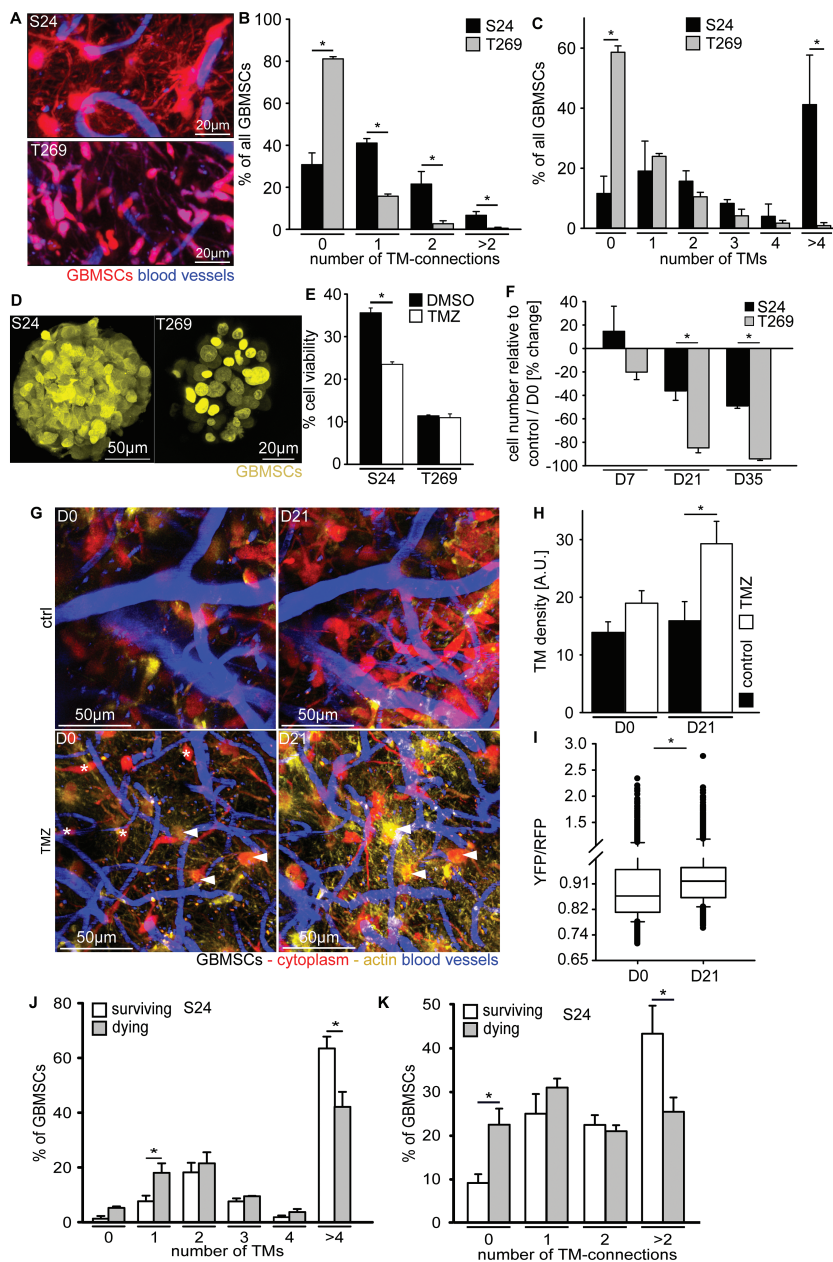


**Fig. 5** TM connectivity and resistance to chemotherapy. (A) Representative images of S24 and T269 GBMSCs showing a higher number of long TMs in S24 than in T269, 64 ± 4 days after tumor implantation, 3D images, 42–72 μm under the brain surface. (B) Number of TM connections and (C) number of TMs per GBMSC in mouse gliomas originating from S24 vs T269 GBMSCs (3 regions in n = 3 animals per group, 31–80 cells, 69–99 μm under brain surface, t-test). (D) Representative confocal in vitro images of S24 and T269 spheroids, demonstrating the absence of relevant TMs in vitro. (E) Quantification of these GBMSC lines in vitro shows a lower cell viability of S24 cells under TMZ treatment, while T269 cells are not significantly affected after 96 hours of incubation (MTT assay, n = 3 per group, t-test). (F) Tumor cell regression in vivo after 3 days of TMZ treatment is extensive in T269 tumors, but only moderate in S24 tumors (2 regions in n = 3 mice per group, rank sum test). (G) S24 GBMSCs with a high number of TMs and high TM connectivity to other tumor cells (arrowheads) preferentially survive the cytotoxic effects of TMZ chemotherapy, while non-TM-connected cells (asterisks) preferentially die the weeks after. Representative in vivo MPLSM maximum intensity projections, 30–150 μm depth under the brain surface. Note the relative increase in TMs and yellow fluorescence in the treatment group vs control group, the latter indicating an increased content of actin (LifeAct YFP)-rich TMs compared with the red fluorescence of tumor cell cytoplasm (tdTomato). (H) The number of TMs per GBMSC increases 21 days after TMZ treatment vs controls (S24, 231–2520 TMs from n = 3 mice, one-way ANOVA). (I) YFP(Actin)/red fluorescent protein(cytoplasm) signal ratio on D0 and 21 days after TMZ (S24, 3375–5080 tumor cell structures from 2 regions in n = 3 mice, t-test). (J, K) Percentage of the number of glioblastoma cells that survive for a long period of time (62 days) or die after TMZ treatment, in relation to their number of TMs (J) or TM-mediated interconnection to other tumor cells on day zero (K) (26–353 tumor cells from 2 regions in n = 3 mice per group, t-test). Error bars show SEM. \*P < 0.05.



the T269 cell line (Fig. 5E). In sharp contrast, when in vivo therapy effects of TMZ on S24- and T269-derived gliomas were quantified, the TM-rich and TM-interconnected S24 GBMSCs were much more resistant to TMZ than the TM-poor T269 cells (Fig. 5F). Mice with both S24 and T269 gliomas lived significantly longer after TMZ than control animals; however, in line with the tumor effects, the survival benefit appeared more pronounced in the T269 group (Supplementary Figure S2A, B).

Next we sought to analyze whether highly TM-connected glioblastoma cells within one single tumor were more likely to survive treatment with TMZ. This analysis was possible for S24-derived mouse gliomas, where the number of strongly TM-connected tumor cells was high enough (Fig. 5A): while TM-connected tumor cells survived (Fig. 5G, arrowheads), nonconnected ones disappeared after TMZ chemotherapy (Fig. 5G, asterisks). Sixty-two days after TMZ treatment, only a small percentage of glioblastoma cells that were already present at day 0 survived; most cells died (Supplementary Fig. 2C, D). A deeper analysis of the surviving GBMSCs confirmed that those tumor cells that extended more than 4 TMs and were connected to multiple other GBMSCs with their TMs were more likely to survive TMZ, while the TM-devoid, unconnected tumor cells were more likely to disappear after TMZ (Fig. 5J, K). The total tumor density of TMs increased after TMZ treatment, compared with controls (Fig. 5H), as well as the actin content of tumor cell structures (Fig. 5I). TMs are known to be particularly actin rich.<sup>23</sup>

Together this implies a role of TM-mediated glioma cell connectivity for primary, and potentially also adaptive, resistance to alkylating chemotherapy.

## Discussion

Here we demonstrate that the formation of TMs contributes to recurrence after surgery and resistance against chemotherapy in a mouse model of GB. Primary and/or adaptive resistance against standard therapies results in inevitable disease recurrence in GB, making the targeting of resistance mechanisms a plausible avenue for therapy development. The findings of this study, performed in a refined intravital imaging model of the disease, demonstrates that surgical lesions are specifically and excessively repopulated in a TM-dependent manner by glioblastoma cells and that this “repair” mechanism is largely inhibited when GAP-43 is knocked down, leading to a deficient TM formation. Moreover, TMs also contribute to resistance against chemotherapy, as TM-connected tumor cells and TM-rich tumors are more likely to resist TMZ treatment.

Macro- and/or denser microscopic tumor remains at the resection margin were traditionally held accountable for the predominantly local recurrence pattern after surgery in malignant gliomas,<sup>9,10,12</sup> and the reduction of these remains by extensive surgery was seen as the main reason why progression-free and overall survival of patients positively correlated with the extent of tumor resection in glioblastoma.<sup>78</sup> However, neurosurgeons, neuro-oncologists, and brain tumor biologists alike have hypothesized that a wound healing response of the normal brain at the site

of a surgical injury might actually foster tumor cell proliferation at this very place, finally resulting in local tumor recurrence.<sup>30–32</sup> Reactive astrocytosis around gliomas has been well described,<sup>30,33</sup> and has been linked to increased glioma proliferation and local recurrence patterns after glioma resection in a mouse model,<sup>32</sup> which points to an involvement of the normal brain for local recurrence formation at the resection site. Our study further adds to this concept by demonstrating that glioblastoma cells extend TMs to execute a newly discovered “malignant repair,” replacing the resected parts of the TM-connected tumor cell network, finally greatly exceeding the prior tumor cell density over time.

In other tumor entities outside the brain, local recurrence after microscopically complete resection has also been described and was primarily linked to the release of wound healing factors.<sup>34,35</sup> The hypothesis was that chemoattractants, growth factors, and pro-migratory factors released during the wound healing response after surgical resections were not only driving normal tissue repair, but were also acting as stimuli for cancer cell recruitment and growth.<sup>34–36</sup> Our data support this assumption to some extent, as inhibition of the malignant wound repair is seen with DEX as an anti-inflammatory treatment in the first week. However, this inhibition is only transient, which might be explained by the fact that the inflammatory phase of a brain lesion only lasts for days, not many weeks.<sup>30</sup>

Connection of glioma cells via Cx43 gap junction connections has been shown to protect them from TMZ-induced toxicity in vitro.<sup>37–39</sup> One study has even found an inverse correlation of Cx43 expression and clinical benefits from TMZ chemotherapy in patients.<sup>37</sup> We have previously demonstrated that Cx43 gap junctions can be frequently found within TMs connecting 2 glioma cells as well as between TMs of different glioma cells that cross each other, and that Cx43 expression depends on the ability of glioma cells to form TMs.<sup>23</sup> While Cx43 is expressed highest and most consistently in our primary glioblastoma cell lines, including S24 and T269,<sup>23</sup> other connexins have been described in glioma as well, with often conflicting findings.<sup>40,41</sup> One of these is connexin 46 (Cx46), which has been attributed to tumor growth and self-renewal properties in cancer stem cells.<sup>40</sup> Here we demonstrate for the first time a survival benefit of highly TM-connected glioblastoma cells compared with nonconnected tumor cells after TMZ chemotherapy, and consistently a better therapeutic activity of TMZ on poorly TM-connected gliomas. Together these findings add to a coherent picture where Cx43 gap junction connections within and between intercellular TMs constitute a functional syncytium in which glioma cells are better protected against adverse effects of cytotoxic therapy. The exact mechanisms for this are not entirely clear. It might be that a more even distribution of the small (gap junction permeable) chemotherapeutic agents within the tumor cell network can temporarily prevent critical high drug concentrations for the single tumor cell; it might also be that maintaining a homeostasis of other important intracellular small molecules like Ca<sup>2+</sup> through multicellular exchange could help lower the toxicity of chemotherapy.<sup>23</sup> Finally, it is also possible that nonmalignant brain resident cells like astrocytes might form gap junctions with glioblastoma cells to participate in this protective syncytium<sup>42,43</sup> and increase tumor cell invasion

and survival.<sup>42,44,45</sup> Similar interactions have been shown in brain metastasis.<sup>43</sup> Besides gap junction coupling, astrocytes can secrete growth factors that might trigger tumor cell proliferation and invasion.<sup>32</sup> Nevertheless, by undermining the formation of functional, GAP-43-dependent and typically Cx43-bearing TMs with TM-targeting drugs that still need to be developed or discovered, it is possible that glioma cells can be further sensitized to TMZ treatment, at least those with *MGMT* promoter hypermethylation. In this subgroup, TM number and/or interconnectivity in patient tumor samples should be explored as a potential additional predictive biomarker for TMZ response, adding to the well-established *MGMT* promoter methylation status.

In conclusion, the different biological functions of TMs seem to be involved in primary and adaptive resistance of GB to all standard treatment modalities. Thus, pharmacological inhibition of TMs could be a new approach to lower resistance and recurrence rates of GB. Postsurgical TM-targeting strategies, including locally applied drugs left in the resection cavity, emerge as an interesting strategy that should be tested for prevention of local recurrences. Furthermore, to reduce TMZ resistance, pharmacological inhibition of TM function and stability, and of TMZ-induced increase in TM formation, might be most effective when applied concomitantly to TMZ.

## Supplementary Material

Supplementary material is available at *Neuro-Oncology* online.

### Funding

This work was supported by Deutsche Forschungsgemeinschaft (DFG WI 1930/5-1 to F.W.) and a Heinrich F. C. Behr Stipendium to S.W.

### Acknowledgments

We thank P. Brastianos for reading and commenting on the manuscript, J. Blaes for cell transductions, F. Sahm for the 450k analysis, M. Gömmel and T. Schmenger for technical assistance and advice, and P. Rübmann for technical assistance.

**Conflict of interest statement.** No competing financial interests.

## References

- Weller M, Wick W, Aldape K, et al. Glioma. *Nat Rev Dis Primers*. 2015; 1:15017.
- Stupp R, Mason WP, van den Bent MJ, et al.; European Organisation for Research and Treatment of Cancer Brain Tumor and Radiotherapy Groups; National Cancer Institute of Canada Clinical Trials Group. Radiotherapy plus concomitant and adjuvant temozolomide for glioblastoma. *N Engl J Med*. 2005;352(10):987–996.
- Buckner JC, Shaw EG, Pugh SL, et al. Radiation plus procarbazine, CCNU, and vincristine in low-grade glioma. *N Engl J Med*. 2016;374(14):1344–1355.
- van den Bent M, Erridge S, Vogelbaum M, et al. *Results of the interim analysis of the EORTC randomized phase III CATNON trial on concurrent and adjuvant temozolomide in anaplastic glioma without 1p/19q co-deletion: An Intergroup trial*. Paper presented at: ASCO Annual Meeting 2016; Chicago.
- Sahm F, Capper D, Jeibmann A, et al. Addressing diffuse glioma as a systemic brain disease with single-cell analysis. *Arch Neurol*. 2012;69(4):523–526.
- Scherer H. The forms of growth in gliomas and their practical significance. *Brain*. 1940; 63(1):1–35.
- Stummer W, Pichlmeier U, Meinel T, Wiestler OD, Zanella F, Reulen HJ; ALA-Glioma Study Group. Fluorescence-guided surgery with 5-aminolevulinic acid for resection of malignant glioma: a randomised controlled multicentre phase III trial. *Lancet Oncol*. 2006;7(5):392–401.
- Brown TJ, Brennan MC, Li M, et al. Association of the extent of resection with survival in glioblastoma: a systematic review and meta-analysis. *JAMA Oncol*. 2016;2(11):1460–1469.
- Konishi Y, Muragaki Y, Iseki H, Mitsuhashi N, Okada Y. Patterns of intracranial glioblastoma recurrence after aggressive surgical resection and adjuvant management: retrospective analysis of 43 cases. *Neurol Med Chir (Tokyo)*. 2012;52(8):577–586.
- Petrecca K, Guiot MC, Panet-Raymond V, Souhami L. Failure pattern following complete resection plus radiotherapy and temozolomide is at the resection margin in patients with glioblastoma. *J Neurooncol*. 2013;111(1):19–23.
- Weller M, Cloughesy T, Perry JR, Wick W. Standards of care for treatment of recurrent glioblastoma—are we there yet? *Neuro Oncol*. 2013;15(1):4–27.
- Lemée JM, Clavreul A, Menei P. Intratumoral heterogeneity in glioblastoma: don't forget the peritumoral brain zone. *Neuro Oncol*. 2015;17(10):1322–1332.
- Chowdhary SA, Ryken T, Newton HB. Survival outcomes and safety of carmustine wafers in the treatment of high-grade gliomas: a meta-analysis. *J Neurooncol*. 2015;122(2):367–382.
- Westphal M, Hilt DC, Bortey E, et al. A phase 3 trial of local chemotherapy with biodegradable carmustine (BCNU) wafers (Gliadel wafers) in patients with primary malignant glioma. *Neuro Oncol*. 2003;5(2):79–88.
- Giordano FA, Brehmer S, Abo-Madyan Y, et al. INTRAGO: intraoperative radiotherapy in glioblastoma multiforme—a phase I/II dose escalation study. *BMC Cancer*. 2014;14:992.
- Johnson BE, Mazar T, Hong C, et al. Mutational analysis reveals the origin and therapy-driven evolution of recurrent glioma. *Science*. 2014;343(6167):189–193.
- Wick W, Weller M, van den Bent M, et al. *MGMT* testing—the challenges for biomarker-based glioma treatment. *Nat Rev Neurol*. 2014;10(7):372–385.
- Esteller M, Garcia-Foncillas J, Andion E, et al. Inactivation of the DNA-repair gene *MGMT* and the clinical response of gliomas to alkylating agents. *N Engl J Med*. 2000;343(19):1350–1354.
- Hegi ME, Diserens AC, Gorlia T, et al. *MGMT* gene silencing and benefit from temozolomide in glioblastoma. *N Engl J Med*. 2005;352(10):997–1003.

20. Leu S, von Felten S, Frank S, et al. IDH/MGMT-driven molecular classification of low-grade glioma is a strong predictor for long-term survival. *Neuro Oncol.* 2013;15(4):469–479.
21. Wick W, Hartmann C, Engel C, et al. NOA-04 randomized phase III trial of sequential radiochemotherapy of anaplastic glioma with procarbazine, lomustine, and vincristine or temozolomide. *J Clin Oncol.* 2009;27(35):5874–5880.
22. Wick W, Platten M, Meisner C, et al.; NOA-08 Study Group of Neuro-oncology Working Group (NOA) of German Cancer Society. Temozolomide chemotherapy alone versus radiotherapy alone for malignant astrocytoma in the elderly: the NOA-08 randomised, phase 3 trial. *Lancet Oncol.* 2012;13(7):707–715.
23. Osswald M, Jung E, Sahn F, et al. Brain tumour cells interconnect to a functional and resistant network. *Nature.* 2015;528(7580):93–98.
24. Goslin K, Schreyer DJ, Skene JH, Banker G. Development of neuronal polarity: GAP-43 distinguishes axonal from dendritic growth cones. *Nature.* 1988;336(6200):672–674.
25. Lemke D, Weiler M, Blaes J, et al. Primary glioblastoma cultures: can profiling of stem cell markers predict radiotherapy sensitivity? *J Neurochem.* 2014;131(2):251–264.
26. Kienast Y, von Baumgarten L, Fuhrmann M, et al. Real-time imaging reveals the single steps of brain metastasis formation. *Nat Med.* 2010;16(1):116–122.
27. Winkler F, Kienast Y, Fuhrmann M, et al. Imaging glioma cell invasion in vivo reveals mechanisms of dissemination and peritumoral angiogenesis. *Glia.* 2009;57(12):1306–1315.
28. Winkler F, Kozin SV, Tong RT, et al. Kinetics of vascular normalization by VEGFR2 blockade governs brain tumor response to radiation: role of oxygenation, angiopoietin-1, and matrix metalloproteinases. *Cancer Cell.* 2004;6(6):553–563.
29. Deutsch MB, Panageas KS, Lassman AB, Deangelis LM. Steroid management in newly diagnosed glioblastoma. *J Neurooncol.* 2013;113(1):111–116.
30. Hamard L, Ratel D, Selek L, Berger F, van der Sanden B, Wion D. The brain tissue response to surgical injury and its possible contribution to glioma recurrence. *J Neurooncol.* 2016;128(1):1–8.
31. Ratel D, van der Sanden B, Wion D. Glioma resection and tumor recurrence: back to Semmelweis. *Neuro Oncol.* 2016;18(12):1688–1689.
32. Okolie O, Bago JR, Schmid RS, et al. Reactive astrocytes potentiate tumor aggressiveness in a murine glioma resection and recurrence model. *Neuro Oncol.* 2016;18(12):1622–1633.
33. Kolar K, Freitag-Andrade M, Bechberger J, et al. Podoplanin: a marker for reactive gliosis in gliomas and brain injury. *J Neuropathol Exp Neurol.* 2014; 74(1):64–74.
34. Ekblad L, Lindgren G, Persson E, Kjellén E, Wennerberg J. Cell-line-specific stimulation of tumor cell aggressiveness by wound healing factors—a central role for STAT3. *BMC Cancer.* 2013;13:33.
35. Mannino M, Yarnold J. Effect of breast-duct anatomy and wound-healing responses on local tumour recurrence after primary surgery for early breast cancer. *Lancet Oncol.* 2009;10(4):425–429.
36. Licitra L, Perrone F, Tamborini E, et al. Role of EGFR family receptors in proliferation of squamous carcinoma cells induced by wound healing fluids of head and neck cancer patients. *Ann Oncol.* 2011;22(8):1886–1893.
37. Murphy SF, Varghese RT, Lamouille S, et al. Connexin 43 inhibition sensitized chemoresistant glioblastoma cells to temozolomide. *Cancer Res.* 2016; 76(1):140–149.
38. Munoz JL, Rodriguez-Cruz V, Greco SJ, Ramkissoon SH, Ligon KL, Rameshwar P. Temozolomide resistance in glioblastoma cells occurs partly through epidermal growth factor receptor-mediated induction of connexin 43. *Cell Death Dis.* 2014;5:e1145.
39. Gielen PR, Aftab Q, Ma N, et al. Connexin43 confers temozolomide resistance in human glioma cells by modulating the mitochondrial apoptosis pathway. *Neuropharmacology.* 2013;75:539–548.
40. Hitomi M, Deleyrolle LP, Mulkearns-Hubert EE, et al. Differential connexin function enhances self-renewal in glioblastoma. *Cell Rep.* 2015;11(7):1031–1042.
41. Sin WC, Crespín S, Mesnil M. Opposing roles of connexin43 in glioma progression. *Biochim Biophys Acta.* 2012;1818(8):2058–2067.
42. Chen W, Wang D, Du X, et al. Glioma cells escaped from cytotoxicity of temozolomide and vincristine by communicating with human astrocytes. *Med Oncol.* 2015;32(3):43.
43. Chen Q, Boire A, Jin X, et al. Carcinoma-astrocyte gap junctions promote brain metastasis by cGAMP transfer. *Nature.* 2016;533(7604):493–498.
44. Sin WC, Aftab Q, Bechberger JF, Leung JH, Chen H, Naus CC. Astrocytes promote glioma invasion via the gap junction protein connexin43. *Oncogene.* 2016;35(12):1504–1516.
45. Lin Q, Liu Z, Ling F, Xu G. Astrocytes protect glioma cells from chemotherapy and upregulate survival genes via gap junctional communication. *Mol Med Rep.* 2016;13(2):1329–1335.